

This is an Open Access document downloaded from ORCA, Cardiff University's institutional repository:<https://orca.cardiff.ac.uk/id/eprint/112618/>

This is the author's version of a work that was submitted to / accepted for publication.

Citation for final published version:

Folli, Andrea , Bloh, Jonathan Zacharias, Armstrong, Katherine Louise, Richards, Emma , Murphy, Damien M. , Lu, Li, Kiely, Christopher , Morgan, David John , Smith, Ronald I, McLaughlin, Abbie C. and Macphee, Donald E. 2018. Improving the selectivity of photocatalytic NO<sub>x</sub> abatement through improved O<sub>2</sub> reduction pathways using Ti<sub>0.909</sub>W<sub>0.091</sub>O<sub>2</sub>N<sub>x</sub> semiconductor nanoparticles: from characterisation to photocatalytic performance. *ACS Catalysis* 8 (8) , pp. 6927-6938. 10.1021/acscatal.8b00521

Publishers page: <http://dx.doi.org/10.1021/acscatal.8b00521>

Please note:

Changes made as a result of publishing processes such as copy-editing, formatting and page numbers may not be reflected in this version. For the definitive version of this publication, please refer to the published source. You are advised to consult the publisher's version if you wish to cite this paper.

This version is being made available in accordance with publisher policies. See <http://orca.cf.ac.uk/policies.html> for usage policies. Copyright and moral rights for publications made available in ORCA are retained by the copyright holders.



# SUPPORTING INFORMATION

## Improving the selectivity of photocatalytic NO<sub>x</sub> abatement through improved O<sub>2</sub> reduction pathways using Ti<sub>0.909</sub>W<sub>0.091</sub>O<sub>2</sub>N<sub>x</sub> semiconductor nanoparticles: from characterisation to photocatalytic performance

Andrea Folli,<sup>\*,†</sup> Jonathan Z. Bloh,<sup>‡</sup> Katherine Armstrong,<sup>†</sup> Emma Richards,<sup>†</sup> Damien M. Murphy,<sup>†</sup> Li Lu,<sup>¶</sup> Christopher J. Kiely,<sup>¶,†</sup> David J. Morgan,<sup>†</sup> Ronald I. Smith,<sup>§</sup> Abbie C. Mclaughlin,<sup>||</sup> and Donald E. Macphee<sup>||</sup>

<sup>†</sup>*School of Chemistry, Cardiff University, Main Building, Park Place, Cardiff CF10 3AT, UK.*

<sup>‡</sup>*DECHEMA Research Institute, Theodor-Heuss-Allee 25, Frankfurt am Main 60468, Germany.*

<sup>¶</sup>*Department of Materials Science and Engineering, Lehigh University, Whitaker Laboratory, 5 East Packer Ave, Bethlehem, PA 18015, USA.*

<sup>§</sup>*ISIS Neutron and Muon Source, STFC Rutherford Appleton Laboratory, Harwell Campus, Didcot OX11 0QX, UK.*

<sup>||</sup>*Department of Chemistry, University of Aberdeen, Meston Building, Meston Walk, Aberdeen AB24 3UE, UK.*

E-mail: folli@cardiff.ac.uk

# Contents

1	X-band CW EPR spectra under irradiation	3
2	Dyson line simulation and analysis	5
	References	6

# 1 X-band CW EPR spectra under irradiation

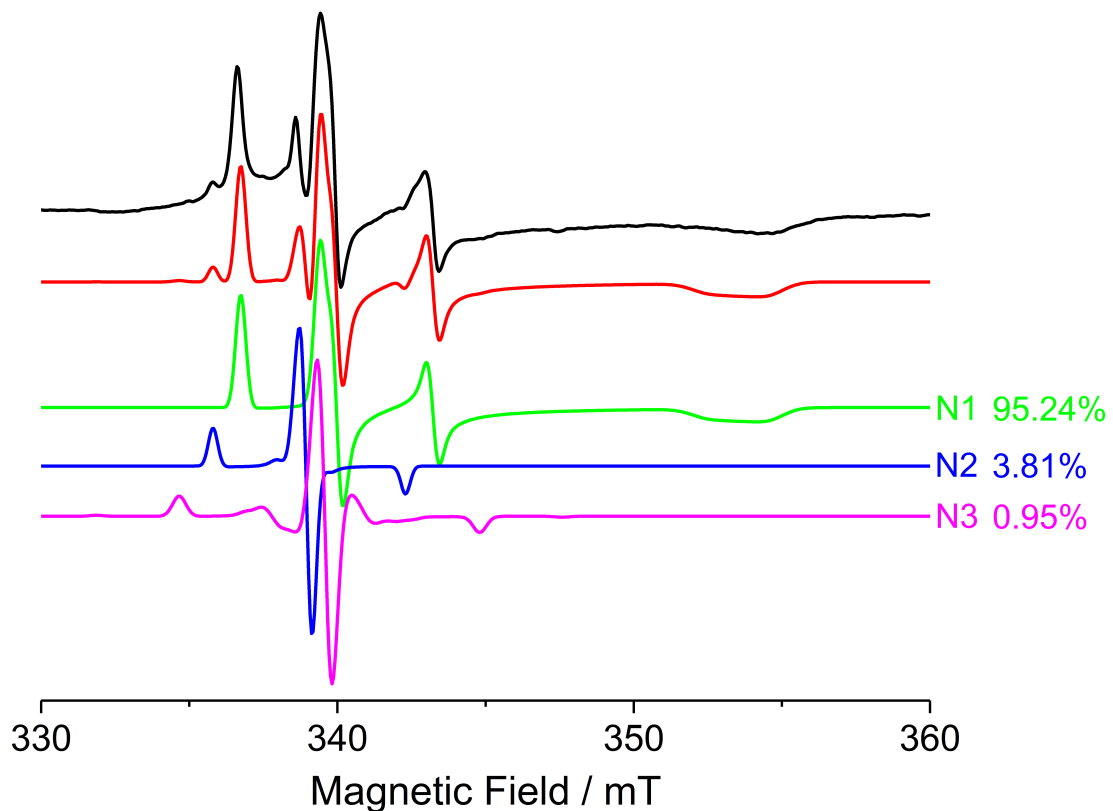


Figure S1: Experimental (black) and simulated (red) X-band CW EPR spectra of the  $\text{Ti}_{0.909}\text{W}_{0.091}\text{O}_2\text{N}_x$  nanoparticles under irradiation with a 455 nm LED light source, measured at 50 K around the free spin region. The simulated spectrum is deconvoluted into its three components N1 (green), N2 (blue) and N3 (magenta). The relative spectral contributions are also reported in the Figure. The experimental spectrum was recorded at 100 kHz field modulation frequency; 0.2 mT field modulation amplitude; 2  $\mu\text{W}$  microwave power and 72 dB receiver gain.

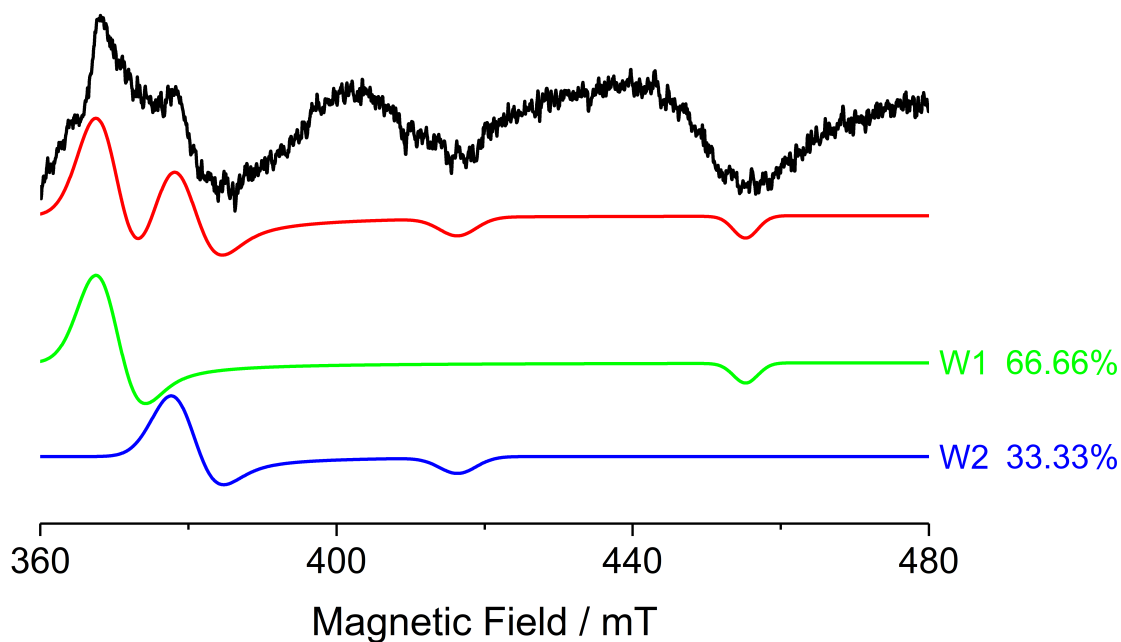


Figure S2: Experimental (black) and simulated (red) X-band CW EPR spectra of the  $\text{Ti}_{0.909}\text{W}_{0.091}\text{O}_2\text{N}_x$  nanoparticles under irradiation with a 455 nm LED light source, measured at 50 K at high fields. The simulated spectrum is deconvoluted into its two components W1 (green), W2 (blue). The relative spectral contributions are also reported in the Figure. The experimental spectrum was recorded at 100 kHz field modulation frequency; 0.2 mT field modulation amplitude; 2  $\mu\text{W}$  microwave power and 72 dB receiver gain.

## 2 Dyson line simulation and analysis

The EPR spectrum at low fields reported in Figure 11 of the main manuscript was simulated using a Dyson function with three parameters:<sup>1</sup>

$$P_D \propto \left[ \frac{\Delta B + \alpha(B - B_0)}{4(B - B_0)^2 + \Delta B^2} + \frac{\Delta B + \alpha(B + B_0)}{4(B + B_0)^2 + \Delta B^2} \right] \quad (\text{S1})$$

that was differentiated with respect to the magnetic field  $B$  to obtain the signal amplitude *s.a.* of the derivative of resonance (first harmonic):

$$s.a. = \frac{dP_D}{dB} \quad (\text{S2})$$

In equation S1,  $\alpha$ , also called asymmetry parameter, represents the ratio of signal amplitude of the left peak A to the right peak B in the derivative of resonance;  $\Delta B$  is the Dyson linewidth and  $B_0$  is the Dyson line position in mT. Simulation was performed as best fit of Equation S2 to the experimental spectrum in Figure 11, from which the optimised parameters (reported in Figure 11)  $\alpha$ ,  $\Delta B$  and  $B_0$  were derived. The fitting was performed using a non-linear least square method based on the Levenberg-Marquardt algorithm, with: function tolerance  $10^{-6}$ , maximum number of iterations 400, maximum function evaluations 1500.

## References

- (1) Popovych, V.; Bester, M.; Stefaniuk, I.; Kuzma, M. Dyson Line and Modified Dyson Line in the EPR Measurements. *Nukleonika* **2015**, *60*, 385–388.